On the Effect of Bandwidth Fragmentation on Blocking Probability in Elastic Optical Networks

Weiran Shi, Zuqing Zhu, *Senior Member, IEEE*, Mingyang Zhang, and Nirwan Ansari, *Fellow, IEEE*

Abstract—In elastic optical networks (EONs), bandwidth fragmentation refers to the existence of non-aligned, isolated and small-sized blocks of contiguous subcarrier slots in the optical spectrum. As they are neither contiguous in the spectrum domain nor aligned along the routing paths, the network operator will have difficulty to use these slots for future connections. In this work, we analyze the effect of bandwidth fragmentation on the blocking probability in EONs. Our theoretical analysis indicates that two factors related to bandwidth fragmentation have effects on the blocking probability: 1) the extent that the available slot-blocks (i.e., blocks of contiguous slots) on different links are aligned on spectrum locations, and 2) the sizes of the available slot-blocks in links' spectra for future requests. When an EON's spectrum becomes more fragmented, the first factor actually reduces the blocking probability, while the second one increases the blocking probability. Their mixed effect determines the overall trend of how the blocking probability will change with bandwidth fragmentation. Our theoretical model can forecast this trend and reveal the relation among the blocking probability, bandwidth fragmentation, request bandwidth distribution, and spectrum utilization. We have also conducted numerical simulations to verify the theoretical analysis, and the simulation results exhibit similar trends as predicted by the theoretical model.

Index Terms—Elastic optical networks, bandwidth fragmentation, blocking probability.

I. INTRODUCTION

NOWADAYS, bandwidth-hungry applications, such as video-on-demand and teleconferencing, have pushed the Internet traffic to grow exponentially and stimulated intensive research on highly scalable and flexible networking technologies. It is known that optical fibers have plenty of bandwidth and therefore play a vital role in the Internet infrastructure. In order to facilitate efficient and agile access to the voluminous bandwidth of optical fibers, researchers have developed technologies such as wavelength-division multiplexing (WDM), optical code-division multiple access (OCDMA), and optical orthogonal frequency-division multiplexing (O-OFDM).

The O-OFDM technology [1] can pack overlapped subcarrier slots in the optical spectrum for high bandwidth efficiency. As a bandwidth-variable O-OFDM transponder can utilize an appropriate number of contiguous subcarrier slots to serve a connection request with the just-enough bandwidth [2], sub-wavelength switching granularity can be achieved in the

W. Shi, M. Zhang, and Z. Zhu are with the School of Information Science and Technology, University of Science and Technology of China, Hefei, Anhui 230027, P. R. China (e-mail: zqzhu@ieee.org).

N. Ansari is with the Department of Electrical and Computer Engineering, New Jersey Institute of Technology, Newark, NJ 07102, USA (e-mail: nirwan.ansari@njit.edu).

optical layer to enable the elastic optical networks (EONs). The flexible nature of EONs imposes sophisticated network planning and provisioning procedures for high-performance operations. To this end, researchers have developed a few routing and spectrum assignment (RSA) algorithms for bandwidth resource allocation [2]–[6]. Since these algorithms manipulate subcarrier slots with bandwidths at a few GHz for RSA, dynamically setting up and tearing down connections can lead to bandwidth fragmentation [7].

Bandwidth fragmentation usually refers to the existence of non-aligned, isolated and small-sized blocks of contiguous subcarrier slots in the spectrum of EONs. As they are neither contiguous in the spectrum domain nor aligned along the routing paths, the network operator will have difficulty to use these slots for future connections. Therefore, people tended to assume that the blocking probability of future requests should increase monotonically with the extent of bandwidth fragmentation [7], [8]. Based on this assumption, previous works have tried to quantify the extent of bandwidth fragmentation with various fragmentation ratios [9], [10] and developed defragmentation methods to reduce the fragmentation ratio to the maximum extent possible [8], [10]–[12]. However, the theoretical analysis on the effect of bandwidth fragmentation on requests' blocking probability is still under-explored. Without solid theoretical validation, the assumption that in EONs, a smaller fragmentation ratio can lead to a lower blocking probability for future connection requests, is still questionable.

In this paper, we perform theoretical analysis on the effect of bandwidth fragmentation on the blocking probability in EONs. Using a commonly-used definition of the fragmentation ratio for EONs [10], [13], we show that a smaller fragmentation ratio may not lead to a lower blocking probability in EONs, especially for small-bandwidth requests, whose blocking probability may actually decrease with the fragmentation ratio. Moreover, our theoretical model reveals the relation among blocking probability, bandwidth fragmentation, request bandwidth distribution, and spectrum utilization, and offers a novel way to forecast how the blocking probability will change with the fragmentation ratio. In order to verify the theoretical analysis, we conduct numerical simulations using the NSFNET topology and various combinations of request bandwidth distribution and spectrum utilization. The results exhibit similar trends as predicted by the theoretical model.

The rest of the paper is organized as follows. Section II describes the theoretical analysis on the effect of bandwidth fragmentation on the blocking probability. Numerical simulations are discussed in Section III, where we verify the theoretical analysis with practical network scenarios. Finally, Section IV summarizes the paper.

II. THEORETICAL ANALYSIS

In this section, we develop a theoretical model to investigate the impact of bandwidth fragmentation on requests' blocking probability in EONs. This model is a simplified description of EON operations, and it may not be able to mimic the realistic operations perfectly. However, it can reveal the nature of the relation among blocking probability, bandwidth fragmentation, request bandwidth distribution, and spectrum utilization.

We assume that in an EON, the bandwidth of each subcarrier slot is unique and each fiber link can accommodate K subcarrier slots at most. The link utilization of a fiber link e is modeled with a bit-mask b_e consisting of K bits. When the j-th slot on e is taken, $b_e[j] = 1$; otherwise, $b_e[j] = 0$.

Definition Let e be a link in an EON, which can accommodate K slots. The link utilization of e is defined as

$$\zeta_e = \frac{sum(b_e)}{K}, \tag{II.1}$$

where $sum(\cdot)$ is the function to add all bits in a bit-mask together.

Definition A slot-block (SB) is a block of one or more contiguous subcarrier slots in the optical spectrum.

As bandwidth fragmentation in EONs is similar to file system fragmentation in computer storage, we borrow the corresponding definition of the fragmentation ratio [13].

Definition Let e be a link in an EON. The bandwidth fragmentation ratio of e is defined as

$$\eta_e = 1 - \frac{1}{n_e}, \tag{II.2}$$

where n_e is the number of available SBs on e.

Note that there are other ways to define the bandwidth fragmentation ratio [9], [10]. Even though they may yield different values (as compared to Eq. (II.2)), their basic principles of quantifying bandwidth fragmentation are similar. Therefore, except for the fragmentation ratio values, there will be no significant difference on the overall trend of the fragmentation's impact on the blocking probability. To this end, we choose the definition in Eq. (II.2) because it is relatively simple and eases the theoretical derivations in this section.

A. Case A

- Two links.
- $\zeta_e = 0.5$.
- Pending request is for 1 slot.

We start the theoretical analysis with a simple network with only two links. We have a pending request for one slot, which needs to use both links. For simplicity, we assume K is an even number, which is the common case in EONs [3]. Let us assume that the link utilizations of both links are identical as $\zeta_e = 0.5, e \in \{e_1, e_2\}$, and the numbers of available SBs for them are also the same as n_e. Then, there are $K \cdot \zeta_e = \frac{K}{2}$ available slots for each link. Fig. 1 illustrates the network status for this case. Here, a red slot means that the slot has already been occupied and is not available, while a white
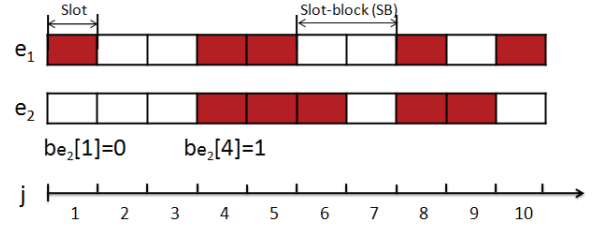

Fig. 1. Network status of an EON that has two links.

slot corresponds to an available slot for pending requests. According to Definition II.2, $n_1 = n_2 = 3, \eta_1 = \eta_2 = \frac{2}{3}$.

For certain link utilization and fragmentation ratio, the available SBs can be distributed for a link in a few feasible ways. We assume that on both links, the available SBs are randomly distributed. When the arrangements of the available SBs for the two links are determined, we can tell whether the pending request for one slot can be served or not. The total number of arrangements is a function of the total number of slots K and the numbers of available SBs for links n_e, when ζ_e is fixed, denoted as

$$M_t = f_t(K, n_e). \tag{II.3}$$

The number of cases that the pending request would be blocked is also a function of K and n_e, denoted as

$$M_b = f_b(K, n_e). \tag{II.4}$$

Therefore, the blocking probability can be calculated as

$$p_b = \frac{M_b}{M_t} = \frac{f_b(K, n_e)}{f_t(K, n_e)}. \tag{II.5}$$

In order to obtain $f_t(K, n_e)$, we take the following procedure. For a given link, under the assumption that there are n_e SBs in it, we can first simplify the problem by ignoring the actual sizes of the SBs (i.e., the numbers of slots). Then, we use $n_e - 1$ unavailable slots to isolate n_e available SBs out. For the rest of the $\frac{K}{2} - (n_e - 1)$ unavailable slots, we organize them into $n_e + 1$ groups. This is because that in order to maintain the number of available SBs as n_e, we have $n_e + 1$ potential locations to insert the unavailable slots in, i.e., $n_e - 1$ locations in between the available SBs and two at the ends. To figure out how many arrangements we can have for these unavailable slots, we introduce the following theorem,

Theorem 2.1: The number of solutions for the equation,

$$x_1 + \cdots + x_j + \cdots + x_J = N, \quad x_j \in \mathbb{Z}, \ x_j \geq 0$$

is: $\begin{pmatrix} N + J - 1 \\ J - 1 \end{pmatrix}$ [14].

In light of *Theorem 2.1*, if we assume that x_i represents the number of unavailable slots that will be inserted at a certain location between two adjacent available SBs, then with $N = \frac{K}{2} - (n_e - 1)$ and $J = n_e + 1$, we get the number of arrangements for the unavailable slots as $\begin{pmatrix} \frac{K}{2} + 1 \\ n_e \end{pmatrix}$, upon which the sizes of the unavailable SBs are determined. Next, we determine the sizes of the available SBs. For the $\frac{K}{2}$ available slots, we organize them into n_e groups. In order
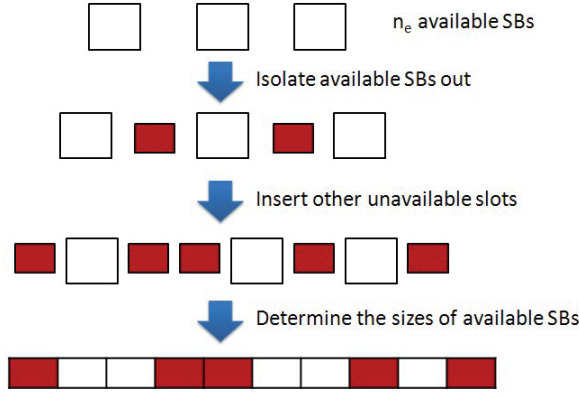
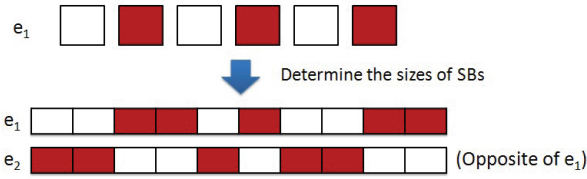Fig. 2. Procedures of formulating f_t for the case with $\zeta_e = 0.5$.

Fig. 3. Procedures of formulating f_b for the case with $\zeta_e = 0.5$.

to maintain the number of available SBs as n_e, we have n_e potential locations to insert the available slots. To figure out how many arrangements we can have for these available slots, we introduce the next theorem.

Theorem 2.2: The number of solutions for the equation,

$$x_1 + \cdots + x_j + \cdots + x_J = N, \quad x_j \in \mathbb{Z}, \ x_j \geq 1$$

is: $\begin{pmatrix} N-1 \\ J-1 \end{pmatrix}$ [14].

Using *Theorem* 2.2 with $N = \frac{K}{2}$ and $J = n_e$, we get the number of arrangements for the available slots as $\begin{pmatrix} \frac{K}{2}-1 \\ n_e - 1 \end{pmatrix}$. Hence, for a link, we have $\begin{pmatrix} \frac{K}{2}+1 \\ n_e \end{pmatrix} \begin{pmatrix} \frac{K}{2}-1 \\ n_e - 1 \end{pmatrix}$ arrangements, and $f_t(K, n_e)$ can be formulated as

$$f_t(K, n_e) = \left[\begin{pmatrix} \frac{K}{2}+1 \\ n_e \end{pmatrix} \begin{pmatrix} \frac{K}{2}-1 \\ n_e - 1 \end{pmatrix} \right]^2. \quad \text{(II.6)}$$

Fig. 2 illustrates an example of the above procedures.

Next, we consider the formulation of $f_b(K, n_e)$. As the pending request is for one slot, it would be blocked if the utilizations of the two links are arranged in such a way that when a slot on one link is available, the corresponding one on the other link is unavailable. Therefore, for all arrangements that lead to blocking, the numbers of available and unavailable SBs have to be the same on both links. There are two scenarios for the SBs after ignoring their sizes. For each scenario (as shown in Fig. 3), we get $\begin{pmatrix} \frac{K}{2}-1 \\ n_e - 1 \end{pmatrix}^2$ arrangements for the slots by following the same procedures discussed above using
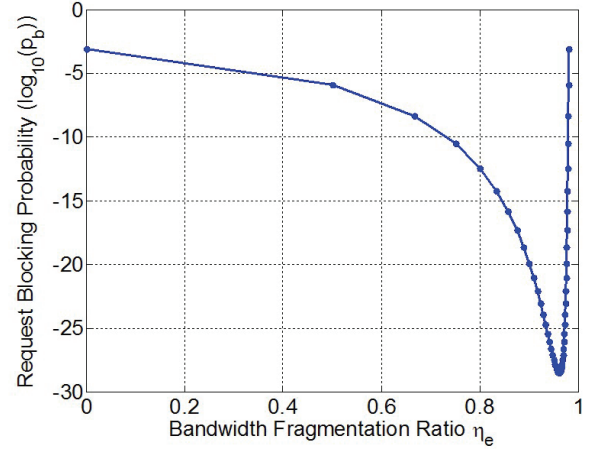

Fig. 4. Blocking probability versus fragmentation ratio for 2 links, $\zeta_e = 0.5$ and a pending request for $\alpha = 1$ slot.

Theorems 2.1 and 2.2. Hence, $f_b(K, n_e)$ can be formulated as

$$f_b(K, n_e) = 2 \begin{pmatrix} \frac{K}{2}-1 \\ n_e - 1 \end{pmatrix}^2. \quad \text{(II.7)}$$

By combining Eqs. (II.6) and (II.7), we get,

$$p_b = \frac{f_b(K, n_e)}{f_t(K, n_e)} = \frac{2}{\begin{pmatrix} \frac{K}{2}+1 \\ n_e \end{pmatrix}^2}. \quad \text{(II.8)}$$

Using Eqs. (II.2) and (II.8), we set $K = 100$ and plot the theoretical results on the blocking probability p_b in Fig. 4. Surprisingly, p_b does not increase monotonically with η_e as assumed in most of the previous works on defragmentation in EONs [8], [10]–[12]. On the contrary, p_b actually decreases with η_e monotonically until $\eta_e = 0.96$ (i.e. $n_e = 25$) and then increases with η_e. This phenomenon can be explained as follows. As the bandwidth of the pending request is the smallest, when the bandwidth utilizations on the links become more fragmented, the probability of having at least one aligned slot on the two links becomes larger initially. When the bandwidth is too fragmented ($\eta_e \to 1$), the probability starts to decrease because the sizes of available SBs on the links approach the bandwidth of the pending request.

The above analysis suggests that in EONs, the blocking probability is related to link utilization, bandwidth fragmentation and distribution of requests' bandwidths. We shall next investigate more complicated cases to verify this proposition.

B. Case B

- Two links.
- $\zeta_e > 0.5$.
- Pending request is for 1 slot.

In this subsection, we investigate the case with $\zeta_e > 0.5$. For this case, the formulation procedure of $f_t(K, n_e)$ is still valid. Since we have $K\zeta_e$ unavailable slots and $K(1 - \zeta_e)$ available slots, the formulation needs to be modified as,

$$f_t(K, n_e) = \left[\begin{pmatrix} K\zeta_e + 1 \\ n_e \end{pmatrix} \begin{pmatrix} K(1 - \zeta_e) - 1 \\ n_e - 1 \end{pmatrix} \right]^2. \quad \text{(II.9)}$$
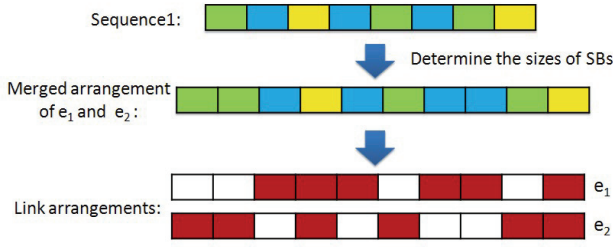
Fig. 5. Procedures of formulating f_b for the case with $\zeta_e > 0.5$.

Since we have $\zeta_e > 0.5$, the argument that for all arrangements that lead to blocking, the numbers of available and unavailable SBs have to be the same on both links, is not valid anymore. Therefore, we need to adopt a new formulation for $f_b(K, n_e)$. In order to find all arrangements that result in request blocking, we define a color-coding scheme as illustrated in Fig. 5. We merge the slot arrangements on the two links to obtain the arrangement along the path. As the pending request for 1 slot will be blocked, there are three slot arrangement scenarios on the two links: 1) a slot on e_1 is available but its corresponding one is not available on e_2, for which we color the slot on the path as green (G); 2) a slot on e_1 is unavailable but its corresponding one is available on e_2, for which we color the slot on the path as blue (B); 3) both slots on e_1 and e_2 are unavailable, for which we color the slot on the path as yellow (Y). Therefore, $f_b(K, n_e)$ equals to the number of arrangements for the G-, B- and Y-slots along the path.

We still assume that the fragmentation ratios of the two links are the same. After ignoring the sizes of the SBs, we reduce the SB arrangement to a sequence, for example,

$$Sequence1: \ G \ B \ G \ B \ G \ Y \ G \ B \ Y \ B \ Y \ B \ G$$

We start the analysis by considering G- and B-SBs and removing Y-SBs temporarily, and *Sequence1* changes to:

$$Sequence2: \ G \ B \ G \ B \ G \ G \ B \ B \ B \ G$$

Note that each "G" or "B" in *Sequence2* corresponds to an SB. Since the number of available SBs on each link is n_e, the numbers of Gs and Bs in *Sequence2* are n_e. To simplify the analysis, we continue to merge adjacent Gs and Bs to form super-SBs, and *Sequence2* further reduces to:

$$Sequence3: \ G \ B \ G \ B \ G \ B \ G$$

Assume that the numbers of G- and B-super-SBs in *Sequence3* are l and s, respectively. Obviously, we have:

$$|l - s| \leq 1 \qquad 1 \leq l \leq n_e, 1 \leq s \leq n_e. \tag{II.10}$$

For *Sequence3*, we define that a G-super-SB has x_j SBs, and a B-super-SB has y_j SBs. Then, we have:

$$x_1 + \cdots + x_j + \cdots + x_l = n_e, \ x_j \in \mathbb{Z}, \ x_j \geq 1 \tag{II.11}$$

$$y_1 + \cdots + y_j + \cdots + y_s = n_e, \ y_j \in \mathbb{Z}, \ y_j \geq 1 \tag{II.12}$$

The number of solutions for Eqs. (II.11) and (II.12) corresponds to the numbers of arrangements for G- and B-SBs in *Sequence2*, respectively. They are, according to *Theorem 2.2*,
$\begin{pmatrix} n_e - 1 \\ l - 1 \end{pmatrix}$ and $\begin{pmatrix} n_e - 1 \\ s - 1 \end{pmatrix}$, respectively.

We then insert Y-slots into *Sequence2* to recover *Sequence1*. The number of Y-slots can be calculated according to ζ_e and K, as $(2\zeta_e - 1)K$. Since we have $2n_e$ SBs in *Sequence2*, there are $2n_e + 1$ intervals for Y-slots. We assume that in the j-th interval, we can insert a Y-SB with z_j slots.

Lemma 2.1: The number of arrangements for inserting Y-SBs into *Sequence2* equals to the number of solutions for the equation:

$$z_1 + \cdots + z_j + \cdots + z_{2n_e+1} = (2\zeta_e - 1)K \\ -(2n_e - s - l), \ z_j \in \mathbb{Z}, \ z_j \geq 0. \tag{II.13}$$

Proof: The problem of inserting Y-SBs into *Sequence2* can be first modeled by the following equation:

$$z_1 + \cdots + z_j + \cdots + z_{2n_e+1} = (2\zeta_e - 1)K, \ z_j \in \mathbb{Z}. \tag{II.14}$$

According to the procedure for obtaining *Sequence2* from *Sequence1*, we know that there is at least one Y-slot in between two adjacent G-SBs or B-SBs in *Sequence2*. Therefore, we can decompose Eq. (II.14) into an equation array,

$$\begin{cases} z_1^{(1)} + \cdots + z_j^{(1)} + \cdots + z_{J_1}^{(1)} = N_1, \ z_j^{(1)} \in \mathbb{Z}, \ z_j^{(1)} \geq 1 \\ z_1^{(2)} + \cdots + z_j^{(2)} + \cdots + z_{J_2}^{(2)} = N_2, \ z_j^{(2)} \in \mathbb{Z}, \ z_j^{(2)} \geq 0 \\ J_1 + J_2 = 2n_e + 1 \\ N_1 + N_2 = (2\zeta_e - 1)K \end{cases}, \tag{II.15}$$

where $z_j^{(1)}$ represents an interval between two G-SBs or two B-SBs, and $z_j^{(2)}$ represents an interval between a G-SB and a B-SB. After subtracting 1 from each $z_j^{(1)}$ and recombining the equation array, we have

$$z_1 + \cdots + z_j + \cdots + z_{2n_e+1} = (2\zeta_e - 1)K - J_1, \ z_j \in \mathbb{Z}, \ z_j \geq 0.$$

Combining Eqs. (II.11) and (II.12), we have $J_1 = 2n_e - s - l$. Hence, Eq. (II.14) is eventually transformed to

$$z_1 + \cdots + z_j + \cdots + z_{2n_e+1} = (2\zeta_e - 1)K \\ -(2n_e - s - l), \ z_j \in \mathbb{Z}, \ z_j \geq 0.$$

We have thus proved *Lemma* 2.1. ∎

According to *Theorem 2.1*, the number of solutions for Eq. (II.13) is $\begin{pmatrix} (2\zeta_e - 1)K + s + l \\ 2n_e \end{pmatrix}$. We get the number of arrangements for G-, B- and Y-SBs as

$$\gamma(n_e) = \sum_{l=1}^{n_e} \sum_{\substack{|l - s| \leq 1 \\ 1 \leq s \leq n_e}} \begin{pmatrix} n_e - 1 \\ l - 1 \end{pmatrix} \begin{pmatrix} n_e - 1 \\ s - 1 \end{pmatrix} \begin{pmatrix} m \\ 2n_e \end{pmatrix}$$

$$= 2 \left[\sum_{l=1}^{n_e} \begin{pmatrix} n_e - 1 \\ l - 1 \end{pmatrix}^2 \begin{pmatrix} m + l - s \\ 2n_e \end{pmatrix} \right.$$

$$\left. + \sum_{l=1}^{n_e - 1} \begin{pmatrix} n_e - 1 \\ l - 1 \end{pmatrix} \begin{pmatrix} n_e - 1 \\ l \end{pmatrix} \begin{pmatrix} m + l - s + 1 \\ 2n_e \end{pmatrix} \right]. \tag{II.16}$$

Here, $m = (2\zeta_e - 1)K + s + l$. Then, by using the procedures in the previous subsection, we determine the SBs' sizes as

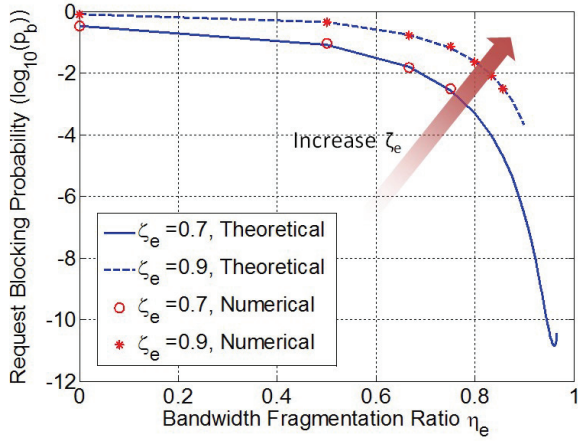$$f_b(K, n_e) = \gamma(n_e) \begin{pmatrix} K(1 - \zeta_e) - 1 \\ n_e - 1 \end{pmatrix}^2. \tag{II.17}$$

Fig. 6.   Blocking probability versus fragmentation ratio for 2 links, $K = 100$, $\zeta_e > 0.5$ and a pending request for $\alpha = 1$ slot.
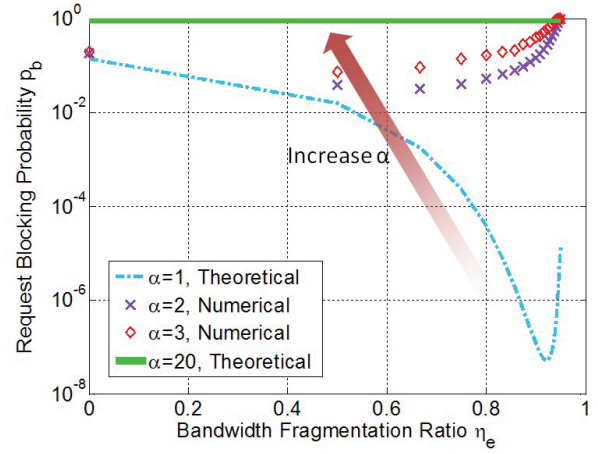

Fig. 7.   Blocking probability versus fragmentation ratio for 2 links, $K = 50$, $\zeta_e = 0.6$ and a pending request for $\alpha \geq 1$ slots.

Finally, by combining Eqs. (II.9) and (II.17), we get the blocking probability for this case as,

$$p_b = \frac{f_b(K, n_e)}{f_t(K, n_e)} = \frac{\gamma(n_e)}{\left(\dfrac{K\zeta_e + 1}{n_e}\right)^2}. \qquad \text{(II.18)}$$

Using Eqs. (II.2) and (II.18), we set $K = 100$, $\zeta_e = 0.7$ and 0.9 and plot the blocking probability p_b versus fragmentation ratio η_e in Fig. 6. In order to verify Eq. (II.18), we also perform Monte Carlo simulations to obtain numerical results on the blocking probability and plot them in Fig. 6. Specifically, we consider a pair of link SB distributions as one case, generate 1,000,000 cases randomly, and obtain the blocking probability by counting the cases in which no common available slots are found on the two links. To maintain sufficient statistical confidence, we only use the simulations to validate p_b that is $\geq 10^{-4}$. As shown in Fig. 6, the theoretical results match well with the numerical ones from the Monte Carlo simulations, with a maximum deviation of 9.21%.

Similar to in Case A, p_b has a trend to first decrease with η_e monotonically and then increases with η_e. When ζ_e is getting larger, which means that more slots in the links are unavailable, the blocking probability p_b gets higher, and the curves end at a smaller value of η_e. For instance, when $\zeta_e = 0.9$, there are only $K \cdot (1 - \zeta_e) = 10$ slots available. So the maximum number of available SBs is 10, and the maximum of η_e is $1 - \frac{1}{10} = 0.9$, at which point the curve would end.

C. Case C

- Two links.
- $\zeta_e > 0.5$.
- Pending request is for multiple slots.

When the pending requests are for multiple slots, the available SBs on the two links do not have to stagger each other completely to result in request blocking. As long as all available SBs on the path are smaller than what the pending request needs, a blocking would happen. To begin with, we define two parameters for a fixed link utilization ζ_e.

Definition Let the bandwidth fragmentation ratio on each link be η_e. The probability that a pending request for α slots would be blocked is $p_b(\eta_e, \alpha)$.

Definition Let the bandwidth fragmentation ratio on each link be η_e. The probability that a pending request for α slots would be blocked, but a request for $\alpha - 1$ slots can be served successfully is $q_b(\eta_e, \alpha)$.

Based on these two definitions, we have:

$$\begin{aligned} p_b(\eta_e, 1) &= q_b(\eta_e, 1) \\ p_b(\eta_e, 2) &= q_b(\eta_e, 1) + q_b(\eta_e, 2) \\ &\vdots \\ p_b(\eta_e, r) &= \sum_{\alpha=1}^{r} q_b(\eta_e, \alpha). \end{aligned}$$

Obviously,

$$q_b(\eta_e, \alpha) \geq 0, \quad \forall \alpha \geq 1, \qquad \text{(II.19)}$$

which leads to this inequality:

$$p_b(\eta_e, 1) \leq \cdots < p_b(\eta_e, r) \leq \cdots \leq p_b(\eta_e, R+1) = 1, \qquad \text{(II.20)}$$

where R is the total number of available slots on the path. When a pending request's size equals to R, it can be served if and only if $\eta_e = 0$, i.e., there is only one available SB on the path and its size is R. Hence, the curve of $p_b(\eta_e, R)$ is a step function. With this trend, if we continue to decrease the pending request's size, the curve of $p_b(\eta_e, \alpha)$ should first increase monotonically, and then start to have the "decreasing-then-increasing" trend as we plot for $p_b(\eta_e, 1)$ in previous subsections. This phenomenon can be explained as follows:

Two factors related to η_e have effects on p_b: 1) the extent that the available SBs on different links are aligned, and 2) the sizes of the available SBs. The increase of η_e makes the available SBs on a link spread more evenly in the spectrum, and hence the probability of SB-alignments between the links gets larger, which can decrease the blocking probability. However, on the other hand, the increase of η_e also makes the sizes of the available SBs on a link smaller, which can

increase the blocking probability. Therefore, the first factor mainly causes the $p_b(\eta_e, \alpha)$ curve to decrease monotonically, while the second factor mainly leads to an increasing trend. Their mixed effect determines the overall trend of $p_b(\eta_e, \alpha)$.

This analysis can be verified with the two extreme cases discussed above. When the size of the pending request is the smallest as $\alpha = 1$, the first factor plays the major role as one aligned slot is good enough. Therefore, $p_b(\eta_e, 1)$ almost decreases monotonically for all η_e. However, for $p_b(\eta_e, R)$, the second factor plays the major role, because even though the available SBs are aligned, if their sizes are not big enough, the request will still be blocked. Therefore, $p_b(\eta_e, R)$ is a step function. For the cases that $1 < r < R$, when η_e is small and most of the available SBs are larger than r, the $p_b(\eta_e, r)$ curve is mainly affected by the first factor and tends to decrease with η_e, but when the increase of η_e makes most of the available SBs become smaller than r, the second factor dominates and makes the curve increase with η_e. The larger the r is, the smaller the "turning point" is for η_e.

As the analytical formulation of $p_b(\eta_e, \alpha)$ for $\alpha \in (1, R)$ is too complicated to be obtained, we use the Monte Carlo simulation discussed in the previous subsection to obtain p_b. The parameters are $K = 50$, $\zeta_e = 0.6$ and $\alpha = 2$ and 3. Similarly, we generate 1,000,000 cases randomly and record the blocking cases that the pending request cannot be accommodated. The numerical results for $\alpha = 2$ and 3 are plotted in Fig. 7. We also plot the theoretical results for $\alpha = 1$ and 20 ($R = K \cdot (1 - \zeta_e) = 20$) in Fig. 7. The curves in Fig. 7 confirm the discussion above.

D. Case D

- More than two links.
- $\zeta_e > 0.5$.
- Pending request is for multiple slots.

In a real EON, a request may take more than two links. In this subsection, we aim to generalize the analysis for the two-link cases. We define two new parameters for a fixed link utilization ζ_e.

Definition The probability that there is an available SB with α slots located from the j-th slot on a link is $A_j(\eta_e, \alpha)$.

Definition Let η_e be the fragmentation ratio of the links. The probability that a pending request for α slots can be successfully served over h links is $p_s(\eta_e, h, \alpha)$.

With the definitions above and the assumption that the SB distributions on the various links are independent, we have

$$p_s(\eta_e, 1, \alpha) = \sum_{j=1}^{K-\alpha+1} \frac{A_j(\eta_e, \alpha)}{K-\alpha+1},$$

$$p_s(\eta_e, 2, \alpha) = \sum_{j=1}^{K-\alpha+1} \frac{A_j^2(\eta_e, \alpha)}{K-\alpha+1},$$

$$\vdots$$

$$p_s(\eta_e, h, \alpha) = \sum_{j=1}^{K-\alpha+1} \frac{A_j^h(\eta_e, \alpha)}{K-\alpha+1}.$$

Note that for real EON operations, the SB distributions on different links might be correlated, since a request can take two or more links and the corresponding spectrum utilizations on those links should be the same. Nevertheless, as we may also use different routing paths for a source-destination pair in real EON operations, the correlation of SB distributions on different links would not be very strong, especially when the requests can be set up and torn-down dynamically.

We have already analyzed the trend of $1 - p_s(\eta_e, 2, \alpha)$. Here, we will prove that $1 - p_s(\eta_e, h, \alpha)$ follows a similar trend for $h > 2$. We first take an approximation:

$$A_{j_1}(\eta_e, \alpha) \approx A_{j_2}(\eta_e, \alpha), \forall j_1, j_2 \in [3, K - \alpha - 1], \quad \text{(II.21)}$$

which means that the difference between two $A_j(\eta_e, \alpha)$ is negligible when their locations are not at the spectrum edges. This approximation is valid because the spectrum of a fiber link can usually accommodate a lot of slots [3] and $\alpha \ll K$ is usually the case for pending requests, thus making the location of an SB insignificant. Table I shows the numerical results on $A_j(\eta_e, 1)$ with $K = 50$, $\zeta_e = 0.6$ and $\eta_e = 0.875$. We observe that except for $j = 1$, 2, 49, and 50, the values of $A_j(\eta_e, 1)$ are very close with less than 13% deviations. Therefore, we can take one step forward to approximate $p_s(\eta_e, h, \alpha)$ as:

$$p_s(\eta_e, h, \alpha) = \sum_{j=1}^{K-\alpha+1} \frac{A_j^h(\eta_e, \alpha)}{K-\alpha+1} \approx A_{j_0}^h(\eta_e, \alpha), \quad \text{(II.22)}$$

where $A_{j_0}(\eta_e, \alpha) = \max(A_j(\eta_e, \alpha)), \forall j \in [1, K - \alpha + 1]$.

Obviously, $A_{j_0}(\eta_e, \alpha) \in [0, 1]$, and $A_{j_0}(\eta_e, \alpha)^h$, $h \geq 2$ has a monotonically increasing trend in $[0, 1]$. With this fact and Eq. (II.22), we can prove that the trend of $1 - p_s(\eta_e, h, \alpha), h > 2$ follows a similar trend as that of $1 - p_s(\eta_e, 2, \alpha)$. More specifically, the effect of the bandwidth fragmentation ratio η_e on the blocking probability p_b can be generalized from the two-link cases to all cases, i.e., the two factors related to η_e can cause the $p_b(\eta_e, \alpha)$ curve to decrease or increase with η_e, and their mixed effect determines the overall trend of $p_b(\eta_e, \alpha)$. In the next section, we will verify this finding with numerical simulations using a more generic network scenario.

III. NUMERICAL SIMULATIONS

In this section, we perform numerical simulations with the 14-node NSFNET topology in [15] to validate the theoretical analysis in the previous section. In the network, we define the network spectrum utilization ζ and network fragmentation ratio η as the average values of ζ_e and η_e, i.e., $\zeta = mean(\zeta_e)$, $\eta = mean(\eta_e)$. We assume that the bandwidth of a slot is 12.5 GHz, which is a typical value in EONs [3], [5]. If the network is deployed in the C-Band, each fiber link has $\sim$5 THz bandwidth to allocate, which corresponds to 400 subcarrier slots.

We first design numerical simulations to reveal the relation between fragmentation and blocking probability for different link utilizations and request sizes. The simulations generate the network status with certain fragmentation and utilization by controlling the SB distribution on each link artificially. More specifically, we first generate a network status with fixed spectrum utilization ζ and fragmentation ratio η. The network status is obtained by controlling the sizes of available SBs.

TABLE I
RESULTS ON $A_j(\eta_e, 1)$ WITH $K = 50$ AND $\eta_e = 0.875$

j	1	2	3	4	5	6	7	8	9	10
$A_j(\eta_e, \alpha)$	0.2483	0.3573	0.3956	0.3852	0.3991	0.4072	0.4165	0.4130	0.4026	0.4107
j	11	12	13	14	15	16	17	18	19	20
$A_j(\eta_e, \alpha)$	0.3968	0.3852	0.4060	0.4142	0.3944	0.4234	0.4188	0.4200	0.4049	0.4072
j	21	22	23	24	25	26	27	28	29	30
$A_j(\eta_e, \alpha)$	0.3898	0.3805	0.4130	0.4292	0.4118	0.4142	0.4153	0.3921	0.4049	0.4095
j	31	32	33	34	35	36	37	38	39	40
$A_j(\eta_e, \alpha)$	0.4165	0.4095	0.4582	0.4316	0.4142	0.4026	0.3956	0.3933	0.4292	0.4281
j	41	42	43	44	45	46	47	48	49	50
$A_j(\eta_e, \alpha)$	0.4266	0.4188	0.3794	0.3724	0.4037	0.4142	0.4258	0.4049	0.3434	0.2796

We make the sizes of the available SBs follow the normal distribution with mean and variance determined by ζ and η. Then, these available SBs are inserted into the links' spectra randomly. Using this scenario, we can emulate the spectrum utilization in an EON with certain ζ and η. In the next phase, we generate 1,000,000 pending requests, whose source-destination node pairs are randomly chosen. The requests' bandwidths (i.e., α) are randomly distributed within $[1, 6]$ and $[20, 40]$ slots. Finally, we conduct 1,000,000 independent tests to evaluate the blocking performance. In each test, we try to serve one pending request in the network with the generated status, using the shortest-path routing and first-fit spectrum assignment [2]. If the request cannot be accommodated in the generated status, it is marked as blocked. Note that, in addition to the requests' blocking probability p_b, we also obtain the bandwidth blocking probability (BBP), p_{Bb}, because the requests can have different bandwidth requirements. Here, BBP is defined as the ratio of the blocked bandwidth to the total requested bandwidth.

Figs. 8-11 illustrate the simulation results, and respective curves are obtained by curve fitting using the expression of $y = c_0 \cdot exp(c_1 \cdot x)$, where c_0 and c_1 are the fitting constants. As expected, we observe that all three parameters, i.e., network fragmentation ratio η, network spectrum utilization ζ and request bandwidth α, can impact p_b and p_{Bb}. In Fig. 8, p_b decreases with the increase of η because the factor of "the extent that the available SBs on different links are aligned" dominates, while the factor of "the sizes of the available SBs" is not that effective in serving small-bandwidth requests in a relatively empty network. The effect of "the sizes of the available SBs" on p_b can be verified with the simulation scenario shown in Fig. 9, where we purposely make the range of α as 20−40 slots. In Fig. 9, since the factor of "the sizes of the available SBs" is much more pronounced for large-bandwidth requests, we observe that p_b increases with the increase of η even through ζ is lower as compared to the scenarios in Fig. 8. The simulation results for p_{Bb} in Figs. 10-11 show the same trends as those of p_b in Figs. 8-9. It is also interesting to notice that in Figs. 8-11, the results on p_b and p_{Bb} have a relatively large dispersion. Note that with fixed values of η and ζ, we can obtain numerous network statuses in the simulations, due to the complexity of SB distributions. Therefore, even though two points on the figures are close in terms of η, the corresponding network statuses can be quite different, thus incurring certain variations in p_b and p_{Bb}.

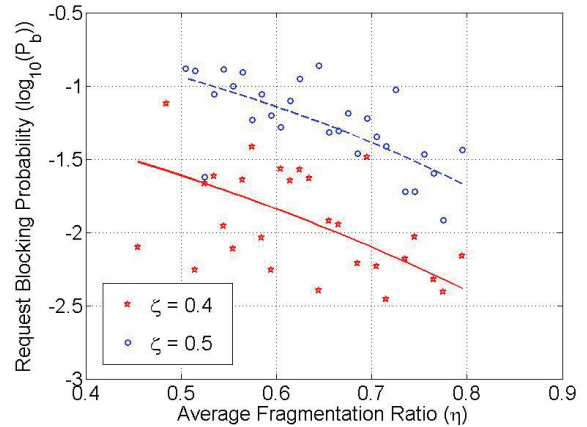The simulation scenario discussed above can reveal the

Fig. 8. Requests' blocking probability versus fragmentation ratio for requests for $\alpha \in [1, 6]$ slots.
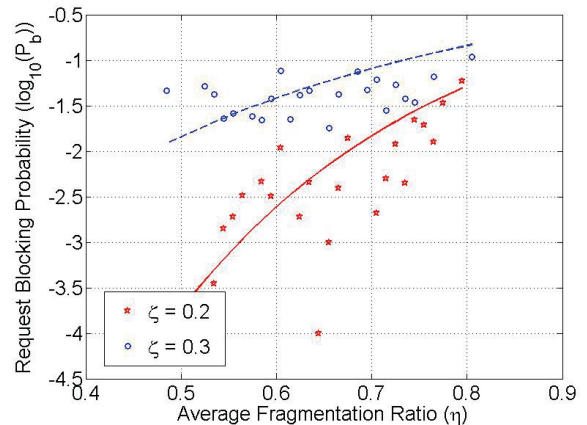

Fig. 9. Requests' blocking probability versus fragmentation ratio for requests for $\alpha \in [20, 40]$ slots.

relation between fragmentation and blocking probability for different link utilizations and request sizes. However, it is rare that all links of an EON have similar fragmentation and utilization. In order to investigate the relation between fragmentation and blocking probability in a realistic network environment, we design another simulation scenario, in which the network status of NSFNET is generated by inserting dynamic requests with 1−6 slots using shortest path routing and first-fit spectrum assignment. The dynamic requests are
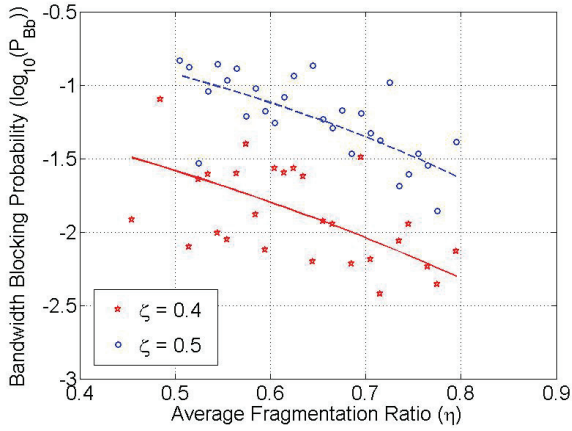
Fig. 10. Requests' bandwidth blocking probability versus fragmentation ratio for requests for $\alpha \in [1, 6]$ slots.
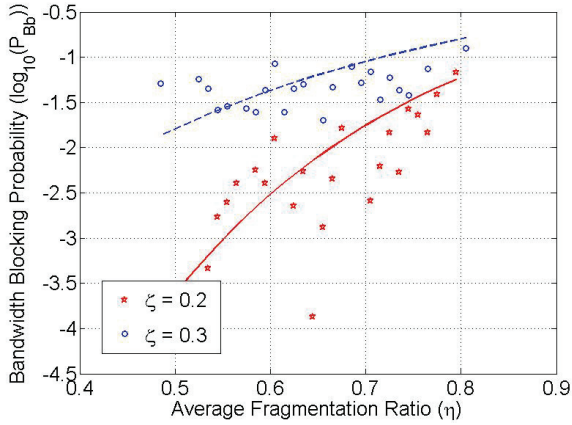

Fig. 11. Requests' bandwidth blocking probability versus fragmentation ratio for requests for $\alpha \in [20, 40]$ slots.

generated with the Poisson traffic model. Then, we perform numerous simulations by changing the traffic load, collect the results on average utilization, average fragmentation ratio, and BBP (i.e., $\{\zeta, \eta, p_{Bb}\}$), and obtain Fig. 12. The numbers on the contours in Fig. 12, obtained by interpolating the original simulation results, are BBP. It can be seen that when we fix ζ at 0.25, p_{Bb} decreases with the increase of η. However, if we increase ζ to 0.3, the "decreasing-then-increasing" trend of p_{Bb} with the increase of η can be observed.

The simulation results in Figs. 8-9 illustrate that the EON's request blocking probability p_b can decrease with the increase of fragmentation ratio η for small-bandwidth requests, i.e. $\alpha \in [1, 6]$ or the bandwidth requirement is $12.5-75$ Gb/s if we assume that one slot can carry 12.5 Gb/s with BPSK. Meanwhile, we notice that a 12.5-GHz slot can easily carry 25 Gb/s or even 50 Gb/s capacity with more advanced modulation schemes, such as QPSK or 8-QAM [2], [3]. Therefore, the actual bandwidth can be larger than 100 Gb/s for these "small-bandwidth" requests, if the advanced modulation schemes are used. Consider that future EONs can carry requests with various bandwidth requirements, we can see that a network operator, though can employ defragmentation to reduce the
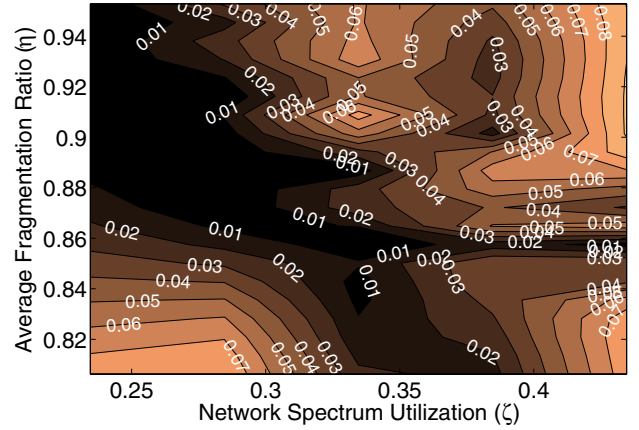

Fig. 12. Contours of BBP p_{Bb} versus spectrum utilization ζ and fragmentation ratio η, from simulations using Poisson traffic model and requests for $\alpha \in [1, 6]$ slots in a dynamic EON.

blocking probability, should carefully consider the relation among blocking probability, bandwidth fragmentation, request bandwidth distribution, modulation schemes, and spectrum utilization, and then chooses a proper optimization objective. Moreover, bandwidth fragmentation also exists in the optical networks that are based on flexible-grid WDM [16] or mixed-line-rate [17] WDM technologies. With proper modifications on the model of link spectrum utilization, the method developed in this work can also be utilized to analyze the bandwidth fragmentation issues in those networks.

IV. CONCLUSION

In this paper, we have performed theoretical analysis on the effect of bandwidth fragmentation on the blocking probability in EONs. Our theoretical model reveals that two factors related to bandwidth fragmentation have effects on the blocking probability: 1) the extent that the available SBs on different links are aligned, and 2) the sizes of the available SBs. When the bandwidth becomes more fragmented, the first factor decreases the blocking probability, but the second one pushes the blocking probability to increase. Their mixed effect determines the overall trend of how the blocking probability will change with the fragmentation ratio. Consequently, a smaller fragmentation ratio may not lead to a lower blocking probability in EONs. In order to verify the theoretical results, we have conducted numerical simulations and the results exhibit similar trends as predicted by the theoretical model. Therefore, in employing defragmentation to reduce the blocking probability, a network operator should consider the relation among blocking probability, bandwidth fragmentation, request bandwidth distribution, and spectrum utilization, and then chooses a proper optimization objective.

REFERENCES

[1] W. Shieh, X. Yi, and Y. Tang, "Transmission experiment of multi-gigabit coherent optical OFDM systems over 1000km SSMF fibre," *IEE Electron. Lett.*, vol. 43, pp. 183–185, Feb. 2007.

[2] K. Christodoulopoulos, I. Tomkos, and E. Varvarigos, "Elastic bandwidth allocation in flexible OFDM-based optical networks," *J. Lightw. Technol.*, vol. 29, pp. 1354–1366, May 2011.

[3] M. Jinno *et al.*, "Distance-adaptive spectrum resource allocation in spectrum-sliced elastic optical path network," *IEEE Commun. Mag.*, vol. 48, pp. 138–145, Aug. 2010.

[4] Y. Wang, X. Cao, and Y. Pan, "A study of the routing and spectrum allocation in spectrum-sliced elastic optical path networks," in *Proc. 2011 IEEE INFOCOM*, pp. 1503–1511.

[5] L. Gong, X. Zhou, W. Lu, and Z. Zhu, "A two-population based evolutionary approach for optimizing routing, modulation and spectrum assignments (RMSA) in O-OFDM networks," *IEEE Commun. Lett.*, vol. 16, pp. 1520–1523, Sept. 2012.

[6] Y. Sone *et al.*, "Routing and spectrum assignment algorithm maximizes spectrum utilization in optical networks," in *Proc. 2011 ECOC*, pp. 1–3.

[7] Y. Yin *et al.*, "Dynamic on-demand defragmentation in flexible bandwidth elastic optical networks," *Opt. Express*, vol. 20, pp. 1798–1804, Jan. 2012.

[8] T. Takagi *et al.*, "Disruption minimized spectrum defragmentation in elastic optical path networks that adopt distance adaptive modulation," in *Proc. 2011 ECOC*, pp. 1–3.

[9] X. Wang *et al.*, "Utilization entropy for assessing resource fragmentation in optical networks," in *Proc. 2012 OFC*, pp. 1–3.

[10] M. Zhang *et al.*, "Planning and provisioning of elastic O-OFDM networks with fragmentation-aware routing and spectrum assignment (RSA) algorithms," in *Proc. 2012 ACP*, pp. 1–3.

[11] A. Patel, P. Ji, J. Jue, and T. Wang, "Defragmentation of transparent flexible optical WDM (FWDM) networks," in *Proc. 2011 OFC*, pp. 1–3.

[12] A. Kadohata *et al.*, "Multi-layer Greenfield re-grooming with wavelength defragmentation," *IEEE Commun. Lett.*, vol. 16, pp. 530–532, Apr. 2012.

[13] R. Sears, C. Ingen, and J. Gray, "To BLOB or not to BLOB: large object storage in a database or filesystem?" Tech. Rep. MSR-TR-2006-45, pp. 1–11, Jun. 2006.

[14] R. Brualdi, *Introductory Combinatorics*. Prentice Hall, 2010.

[15] Z. Zhu, W. Lu, L. Zhang, and N. Ansari, "Dynamic service provisioning in elastic optical networks with hybrid single-/multi-path routing," *J. Lightw. Technol.*, vol. 31, pp. 15–22, Jan. 2013.

[16] A. Patel, P. Ji, J. Jue, and T. Wang, "Hierarchical multi-granular switching in flexible grid WDM networks," in *Proc. 2012 OFC*, pp. 1–3.

[17] M. Batayneh *et al.*, "On routing and transmission-range determination of multi-bit-rate signals over mixed-line-rate WDM optical networks for carrier Ethernet," *IEEE/ACM Trans. Netw.*, vol. 19, pp. 1304–1316, Oct. 2011.

Weiran Shi is an undergraduate student at the School of Information Science and Technology, University of Science and Technology of China, Hefei, China. She is expected to graduate in July 2013. Her research interest is bandwidth fragmentation in elastic optical networks.

Zuqing Zhu (M'07-SM'12) received the PhD degree from the Department of Electrical and Computer Engineering, University of California, Davis, in 2007. From Jul. 2007 to Jan. 2011, he worked in the Service Provider Technology Group of Cisco Systems, San Jose, as a senior R&D engineer. In Jan. 2011, Dr. Zhu joined the University of Science and Technology of China (USTC), where he currently is an Associate Professor. His research interests are optical networks, energy-efficient networks, and cloud computing. He has published more than 80 papers in peer-reviewed journals and conferences of IEEE, IEE and OSA. Dr. Zhu has been in the technical program committees (TPC) of INFOCOM, ICC, GLOBECOM, ICCCN and etc. Dr. Zhu was a guest editor of *IEEE Network* special issue on "Optical Networks in Cloud Computing". Dr. Zhu is also an editorial board member of *Elsevier Journal of Optical Switching and Networking* (OSN), *Springer Telecommunication Systems Journal* (TSMJ), *Wiley European Transactions on Emerging Telecommunications Technologies* (ETT), and etc. He is a Senior Member of IEEE and a Member of OSA.

Mingyang Zhang (S'12) received the B.S. degree from the Department of Electrical Engineering, Harbin Institute of Technology, Harbin, China, in 2012. He is working toward his M.S. degree at the School of Information Science and Technology, University of Science and Technology of China, Hefei, China. His research interest is elastic optical networks. Mr. Zhang is a Student Member of IEEE.

Nirwan Ansari (S'78-M'83-SM'94-F'09) received BSEE (summa cum laude with a perfect GPA) from NJIT, MSEE from the University of Michigan, Ann Arbor, and Ph.D. from Purdue University, West Lafayette, IN. He joined NJIT in 1988, where he is Professor of Electrical and Computer Engineering. He has also assumed various administrative positions at NJIT. He was Visiting (Chair/Honorary) Professor at several universities. His current research focuses on various aspects of broadband networks and multimedia communications.

Prof. Ansari has served on the Editorial/Advisory Board of eight journals. He was elected to serve in the IEEE Communications Society (ComSoc) Board of Governors as a member-at-large (2013-2014) as well as IEEE Region 1 Board of Governors as the IEEE North Jersey Section Chair. He has chaired ComSoc technical committees, and has been actively organizing numerous IEEE International Conferences/Symposia/Workshops, assuming leadership roles as Chair or TPC Chair at various Conferences, Symposia and Workshops.

Prof. Ansari has authored *Computational Intelligence for Optimization* (Springer 1997) with E.S.H. Hou, *Media Access Control and Resource Allocation for Next Generation Passive Optical Networks* (Springer, 2013) with J. Zhang, and edited *Neural Networks in Telecommunications* (Springer 1994) with B. Yuhas. He has also contributed over 400 publications, over one third of which were published in widely cited refereed journals/magazines. He has been granted over fifteen U.S. patents. He has also guest-edited a number of special issues, covering various emerging topics in communications and networking. He has been frequently selected to deliver keynote addresses, distinguished lectures, and tutorials. Some of his recent recognitions include a couple of best paper awards, several Excellence in Teaching Awards, Thomas Alva Edison Patent Award (2010), NJ Inventors Hall of Fame Inventor of the Year Award (2012), and designation as a ComSoc Distinguished Lecturer (2006-2009).